Molecular Structure of 1,2-Dicarba-*closo*-decaborane(10) As Studied by the Concerted Use of Electron Diffraction and ab Initio Calculations†

Drahomír Hnyk,‡ David W. H. Rankin,* and Heather E. Robertson

Department of Chemistry, University of Edinburgh, West Mains Road Edinburgh, EH9 3JJ, U.K.

Matthias Hofmann and Paul von Ragué Schleyer

Institut für Organische Chemie der Universität Erlangen-Nürnberg, Henkestrasse 24, D-91054 Erlangen, Germany

Michael Bühl

Organisch-Chemisches Institut der Universität Zürich, Winterthurerstrasse 190, CH-8057 Zürich, Switzerland

Received February 23, 1994⊗

An electron diffraction study of 1,2-dicarba-*closo*-decaborane (10), 1,2-$C_2B_8H_{10}$, constrained by *ab initio* calculations has been undertaken. A satisfactory refinement ($R_G = 0.052$) was obtained with a bicapped "square" antiprismatic model assuming C_s symmetry. In this structure one carbon atom occupies one of the two capping positions, while the other is adjacent, in a basal position of a "square" pyramid. The experimental molecular dimensions (r_a) are consistent with the r_e structure as derived by the MP2(fc)/6-31G* optimization. The C−C edge [r_a = 153.8(8) pm, r_e = 153 pm] leads to distortion from the regular square pyramidal shape. The compression of the carbon atoms toward the center of the cluster results in a substantial opening of the B(3)C(2)B(5) bond angle [both electron diffraction and MP2(fc)/6-31G* calculations give 95°] from the parent 90°. As a consequence, the C(2)B(3) distance is the longest CB nearest-neighbor separation so far observed in the gas phase, r_a = 179.4(4) pm [cf. r_e = 177.7 pm, MP2(fc)/6-31G*)]. The reliability of the experimental structure is assessed both by IGLO (individual gauge for localized orbitals) calculations of ^{11}B chemical shifts and by MP2(fc)/6-31G* single-point energy calculations.

Introduction

As Štíbr pointed out in his recent review,[1] the chemistry of dicarbaboranes represents the oldest and most investigated area of carbaborane chemistry. This notwithstanding, relatively few structural studies of such compounds have been reported, especially for the important[2] gas-phase molecular geometries. Of the large number of *closo*-, *nido*-, and *arachno*-type dicarbaboranes, $C_2B_{n-2}H_n$, $C_2B_{n-2}H_{n+2}$, and $C_2B_{n-2}H_{n+4}$, the gas-phase structures of the *closo*-systems have been investigated to the greatest extent. Thus, the 1,5-$C_2B_3H_5$,[3] 1,6-$C_2B_4H_6$,[3,4] 1,10-$C_2B_8H_{10}$,[5] and 1,12-$C_2B_{10}H_{12}$[6] molecules, in which the CC unit forms the body-diagonal of the trigonal bipyramid, of the octahedron, of the bicapped square antiprism, and of the icosahedron, respectively, have been characterized structurally by gas-phase electron diffraction (GED). The isomers, in which the two carbon atoms are nearest or next-nearest neighbors, demonstrate geometries with significantly lower symmetry and thus are inherently more difficult for electron diffraction studies. Indeed, only 1,2-$C_2B_4H_6$[7a] and 1,2- and 1,7-$C_2B_{10}H_{12}$,[6] together with the pentagonal bipyramidal 2,4-$C_2B_5H_7$ molecule,[7b] have been studied by GED. No pronounced distortion from regular icosahedral geometries was observed for either 12-vertex species, although only a limited amount of structural information was provided.

The reliability of the electron-diffraction structures of the two isomeric $C_2B_4H_6$ compounds with respect to their computed geometries (3-21G, 6-31G*, and MP2/6-31G* levels) has been assessed recently by the combined *ab initio*/IGLO[8]/NMR method.[9,10] This has proved to be a very successful tool for structural investigation in the area of polyhedral boron chemistry.[9] In addition to the prediction of the geometric structures of various boranes and heteroboranes,[11] this method has also been used to assist in the analysis of electron-diffraction data.[12]

* To whom correspondence should be addressed.

† A preliminary report of this work was presented at the IMEBORON VIII meeting, Knoxville, TN, July 11−15, 1993.

‡ On leave from the Institute of Inorganic Chemistry of the Academy of Sciences of the Czech Republic, CZ-250 68 Řež near Prague, Czech Republic.

⊗ Abstract published in *Advance ACS Abstracts,* September 1, 1994.

(1) Štíbr, B. *Chem. Rev.* **1992,** *92,* 225.
(2) Hargittai, I.; Hargittai, M. In *Molecular Structures and Energetics*; Liebman, J. F., Greenberg, A., Eds.; VCH Publishers: New York, 1987; Vol. 2, Chapter 1.
(3) McNeill, E. A.; Gallaher, K. L.; Scholer, F. R.; Bauer, S. H. *Inorg. Chem.* **1973,** *12,* 2108.
(4) (a) Mastryukov, V. S.; Dorofeeva, O. V.; Vilkov, L. V.; Zhigach, A. F.; Laptev, V. T.; Petrunin, A. B. *J. Chem. Soc., Chem. Commun.* **1973,** 276. (b) Mastryukov, V. S.; Dorofeeva, O. V.; Vilkov, L. V.; Golubinskii, A. V.; Zhigach, A. F.; Laptev, V. T.; Petrunin, A. B. *Zh. Strukt. Khim.* **1975,** *16,* 171.
(5) Atavin, E. G.; Mastryukov, V. S.; Golubinskii, A. V.; Vilkov, L. V. *J. Mol. Struct.* **1980,** *65,* 259.
(6) Bohn, R. K.; Bohn, M. D. *Inorg. Chem.* **1971,** *10,* 350.
(7) (a) McNeill, E. A.; Scholer, F. R. *Inorg. Chem.* **1975,** *14,* 1081. (b) McNeill, E. A.; Scholer, F. R. *J. Mol. Struct.* **1975,** *27,* 151.
(8) (a) Kutzelnigg, W. *Isr. J. Chem.* **1980,** *19,* 193. (b) Schindler, M.; Kutzelnigg, W. *J. Chem. Phys.* **1982,** *76,* 1919. (c) Kutzelnigg, W.; Schindler, M.; Fleischer, U. *NMR, Basic Principles and Progress*; Springer Verlag: Berlin, New York, 1990; Vol. 23, p 165. (d) Meier, U.; van Wüllen, Ch.; Schindler, M. *J. Comput. Chem.* **1992,** *13,* 551.

0020-1669/94/1333-4781$04.50/0 © 1994 American Chemical Society

Table 1. Nozzle-to-Plate Distances, Weighting Functions, Correlation Parameters, Scale Factors, and Electron Wavelengths

nozzle-to-plate dist/mm	Δs/nm^{-1}	s_{min}/nm^{-1}	sw_1/nm^{-1}	sw_2/nm^{-1}	s_{max}/nm^{-1}	correln param p/h	scale factor k^a	electron wavelength^b/pm
257.36	2	20	40	140	164	0.4872	0.704(6)	5.701
93.77	4	80	10	264	316	0.3643	0.606(13)	5.701

[a] Figures in parentheses are the estimated standard deviations of the last digits. [b] Determined by reference to the scattering pattern of benzene vapor.

In such analyses, the boron−heterovertex framework molecular parameters are prone to significant correlation, with the consequence that several sets of molecular geometries may represent the electron-scattering patterns equally well. Additional information, experimental or theoretical, is thus essential to choose among different geometries. Finally, the differences between geometric parameters computed at a certain level of theory may be applied as constraints during the GED refinements. At the Hartree−Fock level, cluster dimensions are often found to be overestimated with respect to the experimental values,[9c,12a,13] even if the basis set employs polarization functions. For example, a 6-31G* basis set usually leads to overestimates of the B−B bond lengths.

Inclusion of electron correlation effects has been found to be essential for the description of the multicenter bonding. Hence, geometry optimizations are best carried out at the correlated MP2/6-31G* level or higher.

To gain further insight into the structural properties of dicarbaboranes we have undertaken a gas-phase study of 1,2-dicarba-*closo*-decaborane(10), 1,2-$C_2B_8H_{10}$ (**1**, Figure 1), by electron diffraction. As the symmetry of this compound, C_s, is markedly lower than that of the 1,10-isomer, D_{4d} (see Figure 4), the *ab initio* optimized geometry (MP2/6-31G* level) has been used to constrain many parameters, in locating both the C_2B_8 cage and the hydrogen atoms, in the electron-diffraction analysis.[14] The final experimental geometry is supported by IGLO ^{11}B chemical shift (DZ//GED and II'//GED levels) and single-point (MP2/6-31G* level) calculations.

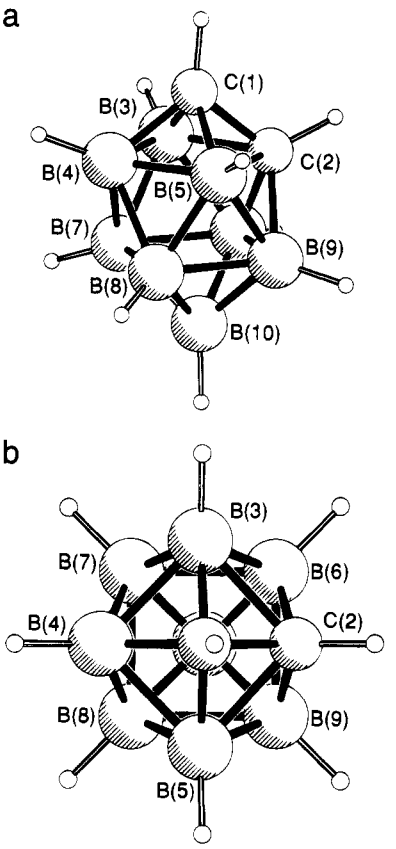

Figure 1. PLUTO plots of different views of the 1,2-$C_2B_8H_{10}$ molecule in the optimum refinement of the electron diffraction data constrained by some MP2/6-31G* differences also showing the atomic numbering of the C_2B_8 body: (a) perspective view; (b) view showing the molecular C_s symmetry.

Experimental and Computational Section

The sample of 1,2-dicarba-*closo*-decaborane(10), prepared according to the literature procedure,[15] was kindly provided by Dr. B. Štíbr (Academy of Sciences of the Czech Republic). The purity was assessed by ^{11}B NMR spectroscopy.

Diffraction patterns were recorded with the Edinburgh gas-diffraction apparatus[16] on Kodak Electron Image plates with a nozzle-tip temperature of about 408 K. The accelerating voltage of the electron beam was about 44.5 kV. Scattering patterns for benzene were also recorded, so that calibration of the electron voltage and nozzle-to-plate distances could be performed. Data were obtained in digital form using the automatic Joyce-Loebl MDM6 microdensitometer at the SERC Laboratory, Daresbury, U.K.[17] The programs used for the data reduction[17] and least-squares refinement,[18] applied to molecular intensities modified by s^4, have been described previously. Published complex scattering factors were employed.[19] The weighting points used in setting up the off-diagonal weight matrix, s ranges, scale factors, correlation parameters, and electron wavelengths are all presented in Table 1.

The geometry was fully optimized in C_s symmetry by standard *ab initio* methods[20] beginning at the SCF level with the 3-21G and 6-31G* basis sets with the CADPAC[21a] program package. Frequency calcula-

(9) For example: (a) Schleyer, P. v. R.; Bühl, M.; Fleischer, U.; Koch, W. *Inorg. Chem.* **1990**, *29*, 253. (b) Bühl, M.; Schleyer, P. v. R. *Angew. Chem., Int. Ed. Engl.* **1990**, *29*, 886. (c) Hnyk, D.; Vajda, E.; Bühl, M.; Schleyer, P. v. R. *Inorg. Chem.* **1992**, *31*, 2464. (d) Mebel, A. M.; Charkin, O. P.; Bühl, M.; Schleyer, P. v. R. *Inorg. Chem.* **1993**, *32*, 463.

(10) Bühl, M.; Schleyer, P. v. R. *J. Am. Chem. Soc.* **1992**, *114*, 477. Many other examples are discussed.

(11) For example: Bausch, J. W.; Prakash, G. K. S.; Bühl, M.; Schleyer, P. v. R.; Williams, R. E. *Inorg. Chem.* **1992**, *31*, 3060.

(12) (a) Hnyk, D.; Bühl, M.; Volden, H. V.; Gundersen, S.; Müller, J.; Paetzold, P. *Inorg. Chem.* **1993**, *32*, 2442. (b) Brain, P. T.; Hnyk, D.; Rankin, D. W. H.; Bühl, M.; Schleyer, P. v. R. *Polyhedron* **1994**, *13*, 1453. (c) Brain, P. T.; Rankin, D. W. H.; Robertson, H. E.; Alberts, I. L.; Schleyer, P. v. R.; Hofmann, M. *Inorg. Chem.* **1994**, *33*, 2565. (d) Hnyk, D.; Brain, P. T.; Rankin, D. W. H.; Robertson, H. E.; Greatrex, R.; Greenwood, N. N.; Kirk, M.; Bühl, M.; Schleyer, P. v. R. *Inorg. Chem.* **1994**, *33*, 2572.

(13) Bühl, M.; Schleyer, P. v. R. In *Electron Deficient Boron and Carbon Clusters*; Olah, G. A., Wade, K., Williams, R. E., Eds.; Wiley: New York, 1991; p 113.

(14) For more information about the molecular orbital constrained electron diffraction, see: Schäfer, L.; Ewbank, J. D.; Siam, K.; Chiu, N.; Sellers, H. L. In *Stereochemical Applications of Gas Phase Electron Diffraction*; Hargittai, I., Hargittai, M., Eds.; VCH: New York, 1988; Part A, pp 301−319.

(15) Rietz, R. R.; Schaeffer, R.; Walter, E. *J. Organomet. Chem.* **1973**, *63*, 1.

(16) Huntley, C. M.; Laurenson, G. S.; Rankin, D. W. H. *J. Chem. Soc., Dalton Trans.* **1980**, 954.

(17) Cradock, S.; Koprowski, J.; Rankin, D. W. H. *J. Mol. Struct.* **1981**, *77*, 113.

(18) Boyd, A. S. F.; Laurenson, G. S.; Rankin, D. W. H. *J. Mol. Struct.* **1981**, *71*, 217.

(19) Ross, A. W.; Fink, M.; Hilderbrandt, R. *International Tables for Crystallography*; Wilson, A. J. C., Ed.; Kluwer Academic Publishers: Dordrecht, The Netherlands, Boston, MA, London, 1992; Vol C, p 245.

Table 2. Ab Initio Optimized Nearest-Neighbor Distances (pm) for 1,2-$C_2B_8H_{10}$

distance	Level of Theory			GED
	3-21G	6-31G*	MP2/6-31G*	
C(1)−C(2)	155.3	152.3	153.0	*153.8(8)*
C(2)−B(3)	183.7	178.1	177.7	*179.4(4)*
C(1)−B(3)	162.3	159.5	160.6	*162.7(4)*
C(1)−B(4)	163.4	160.3	160.4	*162.5(4)*
C(2)−B(6)	173.5	172.2	171.2	*171.8(4)*
B(3)−B(4)	187.2	184.5	183.1	*184.0(4)*
B(3)−B(6)	187.9	184.8	181.2	*181.4(6)*
B(3)−B(7)	181.1	180.3	177.9	*178.3(5)*
B(4)−B(7)	183.4	182.9	180.6	*182.2(16)*
B(6)−B(9)	186.5	183.6	182.8	*184.5(4)*
B(7)−B(8)	188.8	186.8	184.1	*185.8(4)*
B(6)−B(7)	188.6	186.2	183.6	*185.3(4)*
B(6)−B(10)	171.3	169.6	169.8	*170.4(4)*
B(7)−B(10)	173.0	171.1	170.6	*171.2(4)*

tions confirmed the structures to be minima on both potential energy hypersurfaces. The final level of optimization employed was second order Møller−Plesset perturbation theory in the frozen core approximation (denoted as MP2/6-31G*, fc is omitted for simplicity) using the Gaussian 92[21b] program. The three sets of the r_e cluster bond lengths are summarized in Table 2. Chemical shieldings were computed with the IGLO (individual gauge for localized orbitals) program[8] using Huzinaga basis sets:[22] first DZ, i.e. (7s3p) contracted to [4111, 21] for C, B and (3s) contracted to [21] for H, and second II′, i.e. (9s5p1d) contracted to [51111, 2111, 1] for C, B and (3s) contracted to [21] for H. Relative chemical shifts are presented in Table 7. DZ results were obtained with an IGLO lobe version while for II′ calculations the direct IGLO program (DIGLO)[8d] was used.

Molecular Model and Structural Analysis

The *closo*-1,2-$C_2B_8H_{10}$ molecule was assumed to have C_s symmetry. Whereas *closo*-1,10-$C_2B_8H_{10}$ has just three different nearest-neighbor separations, there are 14 such distances in **1**. Three mean distances were chosen as the independent parameters to define the bicapped "square" antiprismatic geometry (see Figure 1): $p_1 = \{r[C(1)-C(2)] + 2r[C(1)-B(3)] + r[C(1)-B(4)]\}/4$, related to the C(1)C(2)B(3)B(4)B(5) "square" pyramid, $p_2 = \{r[B(6)-B(10)] + r[B(8)-B(10)] + r[C(2)-B(6)]\}/3$, related to the B(6)B(7)B(8)B(9)B(10) "square" pyramid and to r[C(2)−B(6)] which is computed to be similar in length to the B(6)−B(10) and B(8)−B(10) distances, and $p_3 = \{r[B(9)-B(6)] + r[B(7)-B(8)] + 2r[B(6)-B(7)] + 2r[C(2)-B(3)]\}/6$, which is the mean value of six of the basal bonds [the B(3)−B(4) bond distance is a dependent parameter in this model]. To complete the description of the C_2B_8 framework, four angular parameters are needed; these were chosen to be the mean angles [B(5)C(2)B(3) + C(2)C(1)B(4)]/2 and [C(1)C(2)X + C(2)XY]/2, where X and Y are the midpoints of the B(6)−B(9) and B(7)−B(8) bonds, respectively, and the differences between these pairs of angles (see Table 3). Since the MP2/6-31G* geometry indicates that the atoms in the B(6)B(7)B(8)B(9) belt are almost perfectly coplanar, this was assumed subsequently in this C_s model. Seven other MP2/6-31G* constraints were also utilized (see Table 3). The five kinds of

Table 3. Molecular Parameters (pm or deg)[a] of 1,2-$C_2B_8H_{10}$ (C_s Symmetry)

p_1	r(CC/CB), [(1-2) + 2(1-3) + (1-4)]/4[b]	160.4(3)
p_2	r(BB), [(6-10) + (8-10) + (2-6)]/3[b]	171.2(4)
p_3	r(CB/BB), [(6-9) + (7-8) + 2(6-7) + 2(2-3)]/6[b]	183.3(4)
p_4	r(BH/CH) (mean)[b]	117.9(4)
p_5	∠[B(5)C(2)B(3) + C(2)C(1)B(4)]/2	99.5[d]
p_6	∠[C(1)C(2)X + C(2)XY]/2[c]	110.6(4)
p_7	∠CCH (mean)[b]	120.5[d]
p_8	∠CBH[b]	121.0[d]
p_9	∠BBH (mean)[b]	124.1(28)
p_{10}	Δr[C(1)−B(3)] − r[C(1)−C(2)]	8.8(10)
p_{11}	Δr[C(1)−B(3)] − r[C(1)−B(4)]	0.2[e]
p_{12}	Δr[C(2)−B(6)] − r[B(8)−B(10)]	0.6[e]
p_{13}	Δr[C(2)−B(6)] − r[B(6)−B(10)]	1.4[e]
p_{14}	Δr[B(7)−B(8)] − r[B(6)−B(9)]	1.3[e]
p_{15}	Δr[B(7)−B(8)] − r[B(6)−B(7)]	0.5[e]
p_{16}	Δr[B(7)−B(8)] − r[C(2)−B(3)]	6.4[e]
p_{17}	Δr(B−H) − r(C−H)	10.3[e]
p_{18}	∠C(2)C(1)B(4) − ∠B(5)C(2)B(3)	9.6[e]
p_{19}	∠C(1)C(2)X − ∠C(2)XY[c]	20.6[e]
p_{20}	∠C(2)C(1)H − ∠C(1)C(2)H	7.4[e]
p_{21}	∠B(10)B(6)H − ∠B(10)B(7)H	5.2[e]
p_{22}	∠B(5)C(2)B(3)[f]	94.7(6)
p_{23}	∠C(2)C(1)B(4)[f]	104.3(6)
p_{24}	∠C(1)C(2)X[c,f]	120.9(4)
p_{25}	∠C(2)XY[c,f]	100.3(4)

[a] Figures in parentheses are the estimated standard deviations of the last digits. [b] For definitions of parameters see text. [c] X,Y are the midpoints of the B(6)−B(9) and B(7)−B(8) bonds, respectively. [d] Refined and fixed in the final refinement. [e] Fixed at the MP2/6-31G* value. [f] Dependent parameter.

computed B−H bond lengths were found to differ by less than 0.5 pm. Consequently, only a single value for all the BH bond lengths, r(B−H), was considered. The same applies to the two kinds of computed C−H bond lengths for which a single value, r(C−H), was thus assumed. Both r(B−H) and r(C−H) were used to define $p_4 = [8r(B-H) + 2r(C-H)]/10$ as one of the independent parameters locating the hydrogen positions. The others are the angles $(CCH)_{mean}$ = [C(1)C(2)H + C(2)C(1)H]/2, (CBH) [the MP2/6-31G* values of the C(1)B(3)H and C(1)B(4)H angles needed in the model were found to be almost the same] and $(BBH)_{mean}$ = [B(10)B(6)H + B(10)B(7)H]/2. In addition to these, the differences between the angles defining the $(CCH)_{mean}$ and $(BBH)_{mean}$ parameters were kept fixed at the MP2/6-31G* values, as was the r(B−H) − r(C−H) difference. The projections of the B(6)−H and B(7)−H bonds onto the B(6)B(7)B(8)B(9) plane were assumed to bisect the B(9)B(6)B(7) and B(8)B(6)B(7) angles, respectively. The B(10)−H bond was assumed to be perpendicular to this plane. The whole structure thus depended on the 21 independent molecular parameters listed in Table 3, of which the 10 most important were refined, some of them only at some point of the analysis.

Refinement of the parameters defining the C_2B_8 framework was straightforward, starting from the MP2/6-31G* values. It was also possible to refine the r[C(1)−B(3)] − r[C(1)−C(2)] constraint, p_{10}, in the final stages of the analysis, giving a value of 8.8(10) pm. This compares well with 7.6 pm obtained by the MP2/6-31G* optimization. The mean value of the B−H and C−H bonds, p_4, refined well, but the angles defining hydrogen positions could not be refined simultaneously; it was thus necessary to fix some of these in the final refinement.

In order to test the possible consequences of the different constraints employed we also tried a model in which the first three parameters were replaced by p_1', p_2', and p_3', being r[C(1)−C(2)], r[(C−B)$_{mean}$], and r[(B−B)$_{mean}$], respectively. The second and the third parameters are the arithmetical mean values of all the C−B and B−B bonds involved in $p_1 - p_3$ and $p_2 - p_3$, respectively, of the original model. The geometrical

(20) Hehre, W.; Radom, L.; Schleyer, P. v. R.; Pople, J. A. *Ab initio Molecular Orbital Theory*; Wiley: New York, 1986.
(21) (a) Amos, R. D.; Rice, J. E.; CADPAC: The Cambridge Analytical Derivatives Package, Issue 4.0. Cambridge, England 1987. (b) Frisch, M. J.; Trucks, G. W.; Head-Gordon, M.; Gill, P. M. W.; Wong, M. W.; Foresman, J. B.; Johnson, B. G.; Schlegel, H. B.; Robb, M. A.; Replogle, E. S.; Gomperts, R.; Andres, J. L.; Raghavachari, K.; Binkley, J. S.; Gonzales, C.; Martin, R. L.; Fox, D. J.; Defrees, D. J.; Baker, J.; Stewart, J. J. P.; Pople, J. A. Gaussian 92, Revision B. Gaussian, Inc., Pittsburgh, PA, 1992.
(22) Huzinaga, S. *Approximate Atomic Wave Functions*; University of Alberta: Edmonton, Canada, 1971.

Table 4. Final Interatomic Distances (r, pm)[a] and Mean Amplitudes of Vibration (u, pm) of 1,2-$C_2B_8H_{10}$

	atomic pair	r_a[b]	u[b]	
d_1	C(1)−C(2)	153.8(8)	4.5[c]	
d_2	C(2)−B(3)	179.4(4)	7.0(2)	
d_3	C(1)−B(3)	162.7(4)	6.0[c]	
d_4	C(1)−B(4)	162.5(4)	6.0[c]	
d_5	C(2)−B(6)	171.8(4)	6.0[c]	
d_6	B(3)−B(4)	184.0(4)[d]	7.0	
d_7	B(3)−B(6)	181.4(6)[d]	7.0	
d_8	B(3)−B(7)	178.3(5)[d]	7.0	
d_9	B(4)−B(7)	182.2(16)[d]	7.0	
d_{10}	B(6)−B(9)	184.5(4)	7.0	tied to u_2
d_{11}	B(7)−B(8)	185.8(4)	7.0	
d_{12}	B(6)−B(7)	185.3(4)	7.0	
d_{13}	B(6)−B(10)	170.4(4)	7.0	
d_{14}	B(7)−B(10)	171.2(4)	7.0	
d_{15}	(C−H)[e]	109.7(4)[f]	7.5[c]	
d_{16}	(B−H)[e]	120.0(4)[g]	7.6(5)	
d_{17}	C(2)···B(4)	249.8(6)[d]	8.3(3)	
d_{18}	C(2)···B(7)	271.3(3)[d]	9.1	
d_{19}	C(2)···B(10)	278.6(8)[d]	9.1	
d_{20}	C(1)···B(6)	275.9(5)[d]	9.1	
d_{21}	C(1)···B(7)	278.0(13)[d]	9.1	
d_{22}	B(3)···B(5)	263.9(6)[d]	9.1	
d_{23}	B(6)···B(8)	261.9(6)[d]	9.1	tied to u_{17}
d_{24}	B(3)···B(8)	284.3(3)[d]	9.1	
d_{25}	B(4)···B(6)	285.7(5)[d]	9.1	
d_{26}	B(4)···B(10)	292.8(14)[d]	9.1	
d_{27}	B(3)···B(10)	290.4(7)[d]	9.1	
d_{28}	B(3)···B(9)	285.6(7)[d]	9.1	
d_{29}	C(1)···B(10)	353.7(9)[d]	8.4(4)	
d_{30}	[C(B)···H][h]	(226 − 282)[d]	12.5(8)	

[a] Other nonbonded B···H, C···H and H···H distances were included in the refinement, but they are not listed here. Their vibrational amplitudes, refined or fixed, were within the range 10−15 pm. [b] Least-squares standard deviations in the last digit are given in parentheses. [c] Fixed. [d] Dependent parameter. [e] See text. [f] The MP2/6-31G* values for the C(1)−H and C(2)−H bond lengths are 108.2 and 108.7 pm, respectively. [g] The MP2/6-31G* values for the five kinds of B−H bonds are as follows (pm): r[B(3)−H], 118.6; r[B(4)−H], 118.7; r[B(6)−H], 118.9; r[B(7)−H], 119.0; r[B(10)−H], 118.6. [h] Two bonds removed.

Table 5. Portion of the Least-Squares Correlation Matrix for 1,2-$C_2B_8H_{10}$ Showing all Elements ≥50% (k_1 and k_2 Are Scale Factors)

p_6	p_9	p_{10}	u_2	k_1	k_2	
−86		−69	62			p_2
−64						p_3
	58					p_4
		86				p_6
				58		u_2
					50	u_{17}

parameters obtained in this refinement were virtually identical, to within one standard deviation, with those based on the original model, and R_G was unchanged. However, a $p_1' - p_3'$ are strongly correlated and this model was not considered further.

The calculated vibrational amplitudes of three cluster-type bonds of *closo*-1,10-$C_2B_8H_{10}$[5] provided the initial values for the refinement of vibrational amplitudes corresponding to the bonded distances defining $p_1 - p_3$ (see above). A single amplitude of vibration was thus employed to characterize the vibration of the bonds within p_2 and p_3, excluding u[C(2)−B(6)], which was fixed as the other bonds (CC, CB) within p_1. The amplitudes of vibration for the bonded C−C distance and for the C−H bonds could not be refined. The parameters

Table 6. Atomic Coordinates (pm) for 1,2-$C_2B_8H_{10}$[a]

atom	x	y	z
	(a) Electron-Diffraction Refinement		
C(1)	0.000	223.982	−132.008
C(2)	0.000	144.972	0.000
B(3,5)	±131.943	129.557	−120.559
B(4)	0.000	109.515	−247.284
B(6,9)	±92.245	0.000	0.000
B(7,8)	±92.895	−33.135	−182.303
B(10)	0.000	−124.412	−71.130
H(11)	0.000	333.475	−138.319
H(12)	0.000	203.575	92.705
H(13,15)	±242.206	176.500	−126.251
H(14)	0.000	138.948	−363.592
H(16,19)	±174.676	−12.265	86.305
H(17,18)	±173.404	−85.280	−254.366
H(20)	0.000	−242.452	−49.676
	(b) *Ab Initio* (MP2/6-31G* Level) Optimization		
C(1)	143.762	80.921	0.000
C(2)	0.000	133.195	0.000
B(3,5)	64.780	32.058	±130.969
B(4)	128.735	−78.787	0.000
B(6,9)	−111.785	41.211	±91.375
B(7,8)	−21.410	−118.576	±92.048
B(10)	−162.708	−92.517	0.000
H(11)	230.051	146.210	0.000
H(12)	−10.388	241.373	0.000
H(13,15)	102.787	70.238	±236.603
H(14)	227.341	−144.885	0.000
H(16,19)	−179.351	101.690	±168.279
H(17,18)	−17.742	−206.327	±127.369
H(20)	−266.950	−149.007	0.000

[a] The hydrogens are numbered in the order of the heavy atoms they are attached to [B(N)−H(N+10)].

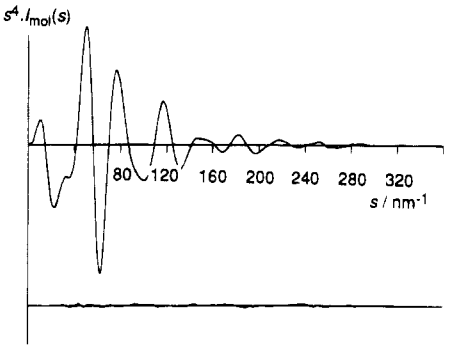

Figure 2. Final experimental molecular-scattering intensities (combined) for 1,2-$C_2B_8H_{10}$. Calculated data have been added to those regions for which experimental data are not available. The weighted difference curve (experimental − theoretical) is also shown.

obtained in the final refinement, for which R_G was 0.052 (R_D = 0.030), are summarized in Table 3. Errors quoted in parentheses are estimated standard deviations obtained in the least-squares refinements. It is not possible to make objective assessment of the effects of possible errors in the computed constraints, and the quoted errors may therefore be somewhat underestimated.

Interatomic distances together with the respective amplitudes of vibration are listed in Table 4 and elements of the least squares correlation matrix exceeding 50% are given in Table 5. Table 6 provides the atomic coordinates for the GED and MP2/6-31G* geometries, from which interatomic distances, bond angles, and dihedral angles of interest may be computed. The combined molecular scattering intensities are shown in Figure 2 while Figure 3 shows the radial distribution curve.

Results and Discussion

The structurally poor radial distribution curve (Figure 3) indicates the difficulty in determining the many parameters

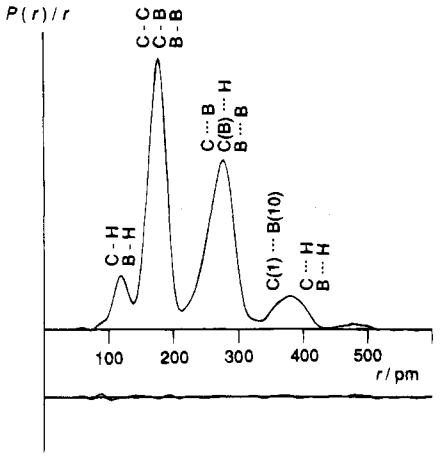

Figure 3. Experimental and difference (experimental − theoretical) radial-distribution curves, $P(r)/r$ against r, for 1,2-$C_2B_8H_{10}$ vapor. Before Fourier inversion, the data were multiplied by $s\exp(-0.00002s^2)/(Z_C - f_C)(Z_B - f_B)$.

necessary to define the full structure. There are three broad peaks at ca. 180, 280, and 300 pm, each of them arising from several component peaks (see Table 4). Although many MP2/6-31G* constraints were employed, the observed parameters reveal valuable information about the shape of the molecule, especially by comparison with parameters for similar compounds. Thus, the presence of the C−C "single" bond [r_a = 153.8(8) pm] brings about a deformation of the C(1)C(2)B(3)B(4)B(5) pyramid from the tetragonal one presented in the 1,10-isomer[5] (see Figure 4). In effect, the carbon atoms are compressed toward the center of the cluster relative to the positions they would have in a regular bicapped square antiprism: this can clearly be seen in Figure 1. As a consequence, the B(3)C(2)B(5) bond angle is opened by ca. 5° from the value of 90° in the parent $B_{10}H_{10}^{2-}$ and in the 1,10-isomer[5] (see Figure 4). Note also that the C(2)−B(3) bond emerges as the longest CB nearest-neighbor separation so far observed in the gas phase[23] [cf. r_a[C(2)−B(3)] = 179 pm, r_e[C(2)−B(3)] = 178 pm]. The deformation of the B(6)B(7)B(8)B(9)B(10) pyramid is much less pronounced. Amplitudes of vibration for nonbonded pairs of atoms are very close to those for nearest neighbors, a very common feature of *closo*-systems.[5,9c,12a]

Magnetic Property Computations. We also performed IGLO calculations employing both the theoretical (3-21G, 6-31G*, and MP2/6-31G*) and the experimental (GED) geometries. The calculated ^{11}B chemical shifts using the geometries are quite similar and show a reasonable fit with experiment (see Table 7). In particular, the shift to high frequency of B(10) [$\delta(^{11}B)$ = 36.5 ppm] with respect to the "parent" $B_{10}H_{10}^{2-}$ [$\delta(^{11}B)$ = −2.0 ppm],[24] is reproduced by the calculations extremely well, regardless of both the geometry and the level of the IGLO calculations used. This shift is known as the antipodal effect,[24] as also observed in the shift of B(10) in *closo*-1-$CB_9H_{10}^-$ of 28.4 ppm, and calculated to be 32.2 ppm at the DZ//3-21G level.[24b] On the other hand, at the DZ level the shift of the B(4) atom tends systematically to exhibit the largest discrepancy between the theoretical and measured $\delta(^{11}B)$ values. As is found for many other carbaboranes,[10] the DZ basis set may not give as satisfactory results as that at higher IGLO levels,

(23) The C−B bond length usually varies within the interval ca. 150−172 pm (see e.g. ref 5 and 10).

(24) (a) Heřmánek, S.; Hnyk, D.; Havlas, Z. *J. Chem. Soc., Chem. Commun.* **1989**, 1859. (b) Bühl, M.; Schleyer, P. v. R.; Havlas, Z.; Hnyk, D.; Heřmánek, S. *Inorg. Chem.* **1991**, *30*, 3107.

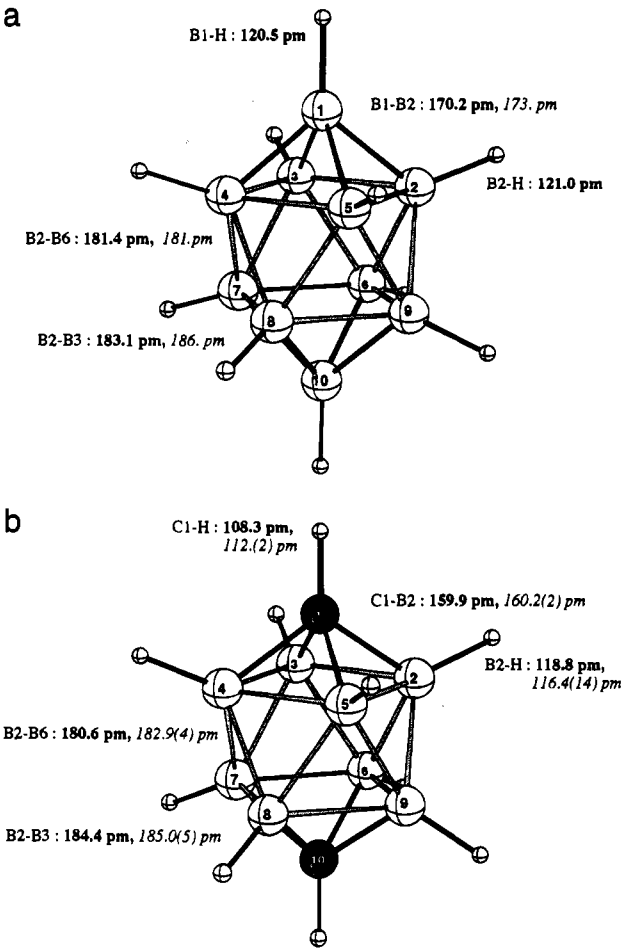

Figure 4. Experimental and theoretical (MP2/6-31G*) geometries of (a) $B_{10}H_{10}^{2-}$ and (b) 1,10-$C_2B_8H_{10}$. Experimental data are given in italics and theoretical parameters (this work) are in bold type. The structure of $B_{10}H_{10}^{2-}$ was determined for the Cu^{2+} salt (Dobrott, R. D.; Lipscomb, W. N. *J. Chem. Phys.* **1962**, *37*, 1779); data for the gas-phase structure of 1,10-$C_2B_8H_{10}$ are taken from ref 5.

Table 7. IGLO Results for 1,2-$C_2B_8H_{10}$

level of theory//geometry	$\delta(^{11}B)^a$ B(3,5)	B(4)	B(6,9)	B(7,8)	B(10)	rel energy[b]/ kJ·mol^{-1}
DZ//3-21G	−14.3	1.1	−18.4	−22.6	36.6	
DZ//6-31G*	−17.1	−0.9	−20.1	−23.9	33.5	
DZ//MP2/6-31G*	−18.3	−2.8	−21.7	−26.9	34.5	
DZ//GED	−15.6	0.2	−21.9	−22.8	35.6	6.3
II′//MP2/6-31G*	−18.3	−5.2	−22.6	−24.4	38.1	
II′//GED	−15.7	−2.0	−22.7	−21.2	39.0	12.1
exptl[c]	*−19.3*	*−8.5*	*−25.4*	*−25.4*	*38.4*	
exptl[d]	*−20.0*	*−9.0*	*−26.1*	*−26.1*	*36.5*	
exptl[e]	*−21.0*	*−10.4*	*−26.8*	*−27.3*	*34.8*	
exptl[f]	*−14.2*	*−5.3*	*−20.7*	*−23.2*	*32.0*	

[a] Relative to $BF_3{\cdot}OEt_2$ (ppm). The $\delta(^{13}C)$ values (ppm) at the DZ//MP2/6-31G* (II′//MP2/6-31G*) level for C(1) and C(2) are 39.9 (32.9) and 49.3 (41.2), respectively. [b] Energy of the GED with respect to the MP2/6-31G* geometry (kJ·mol^{-1}), computed at SCF levels employing DZ and II′ basis sets; the more refined MP2/6-31G* value is 11.3 kJ·mol^{-1} (i.e. MP2/6-31G*//GED vs MP2/6-31G*//MP2/6-31G*). [c] Reference 15. [d] Štíbr, B.; Kennedy, J. D. Personal communication. [e] Heřmánek, S. *Chem. Rev.* **1992**, *92*, 325. [f] 1,2-$(CH_3)_2C_2B_8H_8$.[15]

e.g. basis II′; indeed, basis II′ performs better for all the boron atoms. Note that the smallest difference between the calculated shifts for the B(6,9) and B(7,8) pairs is achieved with the GED geometry. This may be significant, as the corresponding peaks in the experimental spectrum are hardly resolved (Table 7). Interestingly, the IGLO values of **1** also match the experimental

chemical shifts of 1,2-$C_2(CH_3)_2B_8H_8$ satisfactorily (Table 7). This may indicate that the CH_3 groups have very little influence on the cage geometry.

The final experimental geometry of **1** was computed to be only 6.3 kJ·mol^{-1} (DZ basis set) of 12.1 kJ·mol^{-1} (II′ basis set) higher than that of the best theoretical structure (MP2/6-31G*), based on the IGLO-SCF energies. The more refined MP2/6-31G* single-point calculations gave a very close value of 11.3 kJ·mol^{-1}. This energy difference is very well within the range normally observed for experimental structures of boranes and heteroboranes which are believed to be accurate.[10,11] A major part of this "excess energy" may be ascribed to the hydrogen placements. The relative energy was reduced to 2.4 kJ·mol^{-1} when the structure of the C_2B_8 cluster was kept fixed at its experimental geometry and the hydrogen positions were optimized at the MP2/6-31G* level. Both this "energy criterion" and the NMR fit indicate that the electron diffraction parameters afford a reasonable representation of the geometry of 1,2-$C_2B_8H_{10}$, and thus satisfy Beaudet's challenge to solve its molecular structure in his recent review "The Molecular Structures of Boranes and Carboranes".[25]

Acknowledgment. We thank the Science and Engineering Research Council for support of the Edinburgh Electron-Diffraction Service, including provision of microdensitometer facilities at the Daresbury laboratory and research fellowships for D.H. and H.E.R. Finanical support from the Academy of Sciences of the Czech Republic (Grant No 432401) is also highly appreciated. We are indebted to Mr. N. K. Mooljee of the Edinburgh University Computing Service for technical assistance during the course of this work. M.B. thanks Professor W. Thiel and the Alfried Krupp-Stiftung for support. The calculations in Erlangen were performed on a Convex C220S computer and were supported by the Deutsche Forschungsgemeinschaft and the Fonds der Chemischen Industrie. Computer time was granted on a Cray YMP-8 of the Höchstleistungsrechenzentrum Jülich, Jülich, Germany. We thank Professor W. Kutzelnigg, Dr. M. Schindler, Dr. U. Fleischer, and Dr. Ch. van Wüllen for the IGLO and DIGLO programs. We also thank Dr. P. T. Brain and Dr. B. Štíbr for helpful comments.

(25) Beaudet, R. A. In *Advances in Boron and the Boranes*; Liebmann, J. F., Greenberg, A., Williams, R. E., Eds.; VCH Publishers: New York, 1988; Chapter 20, p 417.